

The Journal *of the* CMSC

THE PUBLICATION FOR 3D MEASUREMENT TECHNOLOGY



IN THIS ISSUE:

Targets for Relative Range Error Measurement of 3D Imaging Systems

by Prem Rachakonda, Bala Muralikrishnan, Meghan Shilling, Geraldine Cheok, Vincent Lee, Christopher Blackburn, Dennis Everett, and Daniel Sawyer, NIST

Precision vs. Accuracy Dilemma in Point-Based Rigid-Body Registration

by Marek Franaszek and Geraldine Cheok, NIST

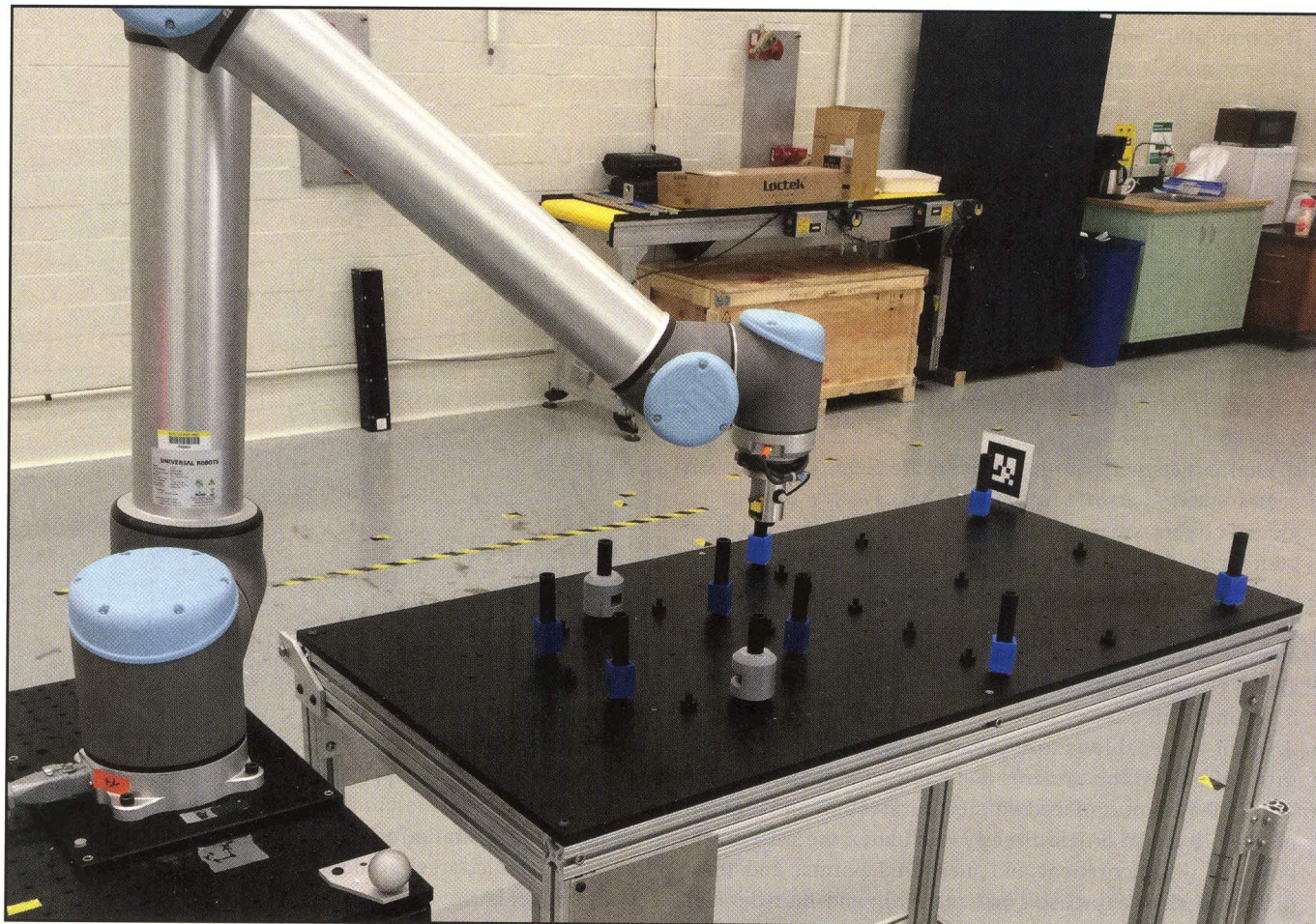
Photogrammetric Measurement of Cabin Bracket Riggings on the Airbus 350

by Jean-Christophe Bry, Airbus Operations SAS, and Nabil Romman, Géodésie Maintenance Services

Dynamic Metrology and ASTM E57.02 Dynamic Measurement Standard

by Roger Bostelman and Tsai Hong, NIST; Steven Legowik, Robotic Research LLC; and Mili Shah, Loyola University Maryland

WWW.CMSC.ORG



Dynamic Metrology and ASTM E57.02 Dynamic Measurement Standard

by Roger Bostelman and Tsai Hong, NIST; Steven Legowik, Robotic Research LLC; and Mili Shah, Loyola University Maryland

Optical tracking systems are used in a wide range of fields, and their market has dramatically increased over the past several years, reaching \$1.2 billion in sales revenue in 2014. This article describes the new ASTM E3064 standard test method procedures for optical tracking systems and will outline the theoretical basis for the analysis of the data from these systems. By way of an example, we will also verify the performance of a 12-camera optical tracking system using these standard procedures and related analysis. An artifact, developed at the National Institute of Standards and Technology (NIST), was verified by a coordinate measuring machine (CMM) and then used in two experiments to verify the test method. This and other in-depth articles are intended to be base references for ASTM E3064.

INTRODUCTION

Optical tracking systems measure the three-dimensional, static, and dynamic position and orientation of multiple markers attached to objects within a measurement space. Optical tracking systems are used in a wide range of fields, including neuroscience,¹ biomechanics,² robotics,³ and automotive assembly.⁴ The market for optical tracking systems has dramatically increased over the past several years, reaching \$1.2 billion in sales revenue in 2014, with annual growth of nearly 53 percent from 2009 to 2014.^{5,6,7}

Potential users of optical tracking systems often have difficulty comparing systems because of the lack of standard performance metrics and test methods, and must therefore rely on vendor claims regarding the system's performance, capa-

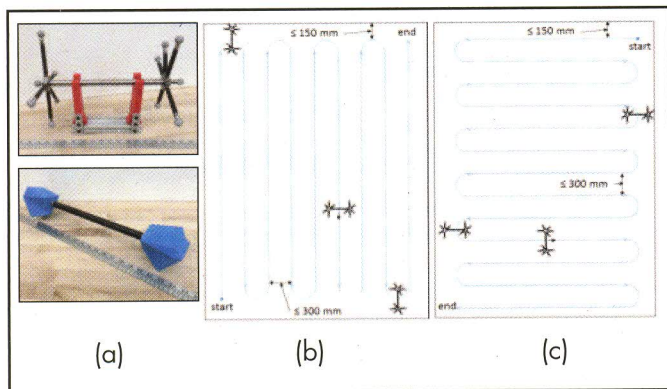


Figure 1. (a) Artifacts to measure optical tracking system performance; (b) forward-back, meaning aligned with the x axis; and (c) side-to-side, meaning aligned with the y axis paths and dimensions for moving the artifact in a test space (reprinted with permission from ASTM E3064-16—"Standard Test Method for Evaluating the Performance of Optical Tracking Systems that Measure Six Degrees of Freedom (6DOF) Pose," copyright ASTM International)

bilities, and suitability for particular applications. The ASTM International Committee E57 on 3D imaging systems' subcommittee on test methods addressed the static performance measurement of optical tracking systems.⁸ Recently, the ASTM E57.02 subcommittee task group has developed a new standard test method, "ASTM E3064 Standard Test Method for Evaluating the Performance of Optical Tracking Systems that Measure Six Degrees of Freedom (6DOF) Pose."⁹ The new test method presents metrics and procedures for measuring, analyzing, and reporting the errors and deviations of dynamic optical tracking systems.

An artifact, developed at NIST and seen in the top portion of figure 1a, was first used to measure a multicamera system and then expanded by the ASTM E57.02 task group to apply to all types of optical tracking systems. The top portion of figure 1a shows an artifact that is used for systems that operate based on active or retroreflective markers; the bottom portion of figure 1a shows an artifact that can be used for systems that use geometric features as markers. The artifact description in the standard allows for a variety of markers to fit the optical tracking system's measurement method. The end markers are measured relative to one another in each right and left cluster on the bar and combined through mathematical analysis to output the resulting bar length throughout the measurement space.

This proposed standard provides a common set of metrics and a test procedure for evaluating the performance of optical tracking systems, and may help to drive improvements and innovations. The standard will also allow users to assess and compare the performance of a candidate optical tracking system and to determine if the measured performance results are within the specifications with regard to the application requirements.

This article describes the new ASTM E3064 standard test method procedures for optical tracking systems, and

will outline the theoretical basis for the analysis of the data from these systems. This project will also verify the performance of a 12-camera optical tracking system as an example. These experiments were conducted using standard procedures, and the analysis method used the artifact seen in the top of figure 1a, which was measured using a CMM. A second method provided in the standard, not mentioned in this article, allows the measurement results to be used without prior knowledge of artifact measurement from a CMM or similar technology. This and other in-depth articles are expected to be the base references for ASTM E57.02.

METRICS AND TEST METHOD

ASTM E3064 provides statistically based performance metrics and a test procedure to evaluate the dynamic performance of optical tracking systems. Measurements from optical tracking systems include inherent positional and orientation angle errors relative to fixed optical measurement components. The metrics are therefore composed of the static and dynamic position and orientation of tracked objects. Metrics are currently being researched that include system latency and maximum dynamic measurement capability, but these are beyond the scope of this article.

The test procedure outlined in E3064 measures the relative pose between two sets of markers that are rigidly attached to the ends of a metrology bar, as seen in figure 1a. The relative pose is then decomposed into positional and angular components, and measurement errors are calculated by comparing results to a known metrology bar length of the artifact.

The artifact includes a metrology bar, 300 mm in length, with markers rigidly attached to each end. This is referred to as a "metrology bar" because it has stiffness and thermal expansion characteristics to allow deflection of less than or

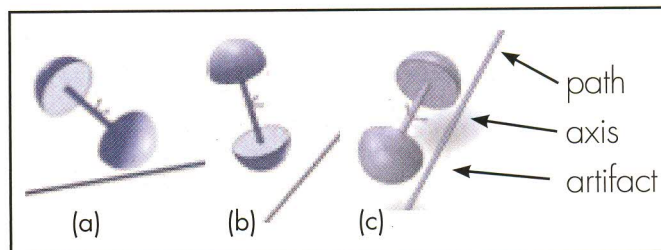


Figure 2. The artifact (shown with axes on the bar centroid) orientations with respect to the path: (a) perpendicular to the path segments in the plane of motion; (b) perpendicular to the path segments and normal to the plane of motion; and (c) in-line with the path segments in the plane of motion; the artifact seen in figure 1a and 1b is oriented with respect to the path as in (a), i.e., perpendicular to the path segments in the plane of motion (this caption includes descriptions directly from E3064 and is reprinted with permission from ASTM E3064-16—"Standard Test Method for Evaluating the Performance of Optical Tracking Systems that Measure Six Degrees of Freedom (6DOF) Pose," copyright ASTM International)

equal to 0.01 mm. Sample metrology bars are made of carbon fiber or titanium and meet the mandatory minimal deflection characteristics. One type of artifact includes two clusters of passive, reflective, spherical (as seen at the top of figure 1a), or active, light-emitting diode (LED) markers located at the ends of the metrology bar. Another form uses reduced pose ambiguity cuboctahedron¹⁰ markers (as seen at the bottom of figure 1a). Both types of markers must be contained within hemispherical volumes of 100 mm maximum radius from the ends of the bar.

The basic procedure for determining the pose measurement error of an optical tracking system first includes rough (hand-held) alignment of the X and Y axes (as seen in figure 1) and the Z axis (aligned with the vertical axis) within the test volume to be measured. The options for the test volume are

- 1) 3,000 mm long \times 2,000 mm wide \times 2,000 mm high
- 2) 6,000 mm long \times 4,000 mm wide \times 2,000 mm high
- 3) 12,000 mm long \times 8,000 mm wide \times 2,000 mm high

The optical tracking system tracks the metrology bar for three trials as it moves throughout the test volume along the two patterns seen in figures 1b and 1c. The metrology bar in each trial corresponds to one of the three orientations seen in figure 2. The centroid of the metrology bar remains at approximately 1 m above the test volume floor and should be moved at approximately the walking speed of 1.2 m/s \pm 0.7 m/s. The metrology bar length is used as a guideline for determining both the distance between the boundary lines and the limits of the test volume. The data from these three trials are then combined into one data set.

The data gathered from the optical tracking system (OTS) consist of the 6DOF pose of the left and right ends of the artifact at time t represented as the homogeneous matrixes:

$${}_{OTS} \hat{H}_{Left}(t) = \begin{bmatrix} \hat{R}_{Left}(t) & \hat{T}_{Left}(t) \\ 0 & 1 \end{bmatrix} \text{ and } {}_{OTS} \hat{H}_{Right}(t) = \begin{bmatrix} \hat{R}_{Right}(t) & \hat{T}_{Right}(t) \\ 0 & 1 \end{bmatrix}$$

The relative pose between the left and right markers is then defined as:

$${}_{Left} \hat{H}_{Right}(t) = {}_{OTS} \hat{H}_{Left}^{-1}(t) {}_{OTS} \hat{H}_{Right}(t) = \begin{bmatrix} \hat{R}_{Left}(t) & \hat{T}_{Left}(t) \\ 0 & 1 \end{bmatrix}^{-1} \begin{bmatrix} \hat{R}_{Right}(t) & \hat{T}_{Right}(t) \\ 0 & 1 \end{bmatrix} = \begin{bmatrix} \hat{R}(t) & \hat{T}(t) \\ 0 & 1 \end{bmatrix}$$

where $\hat{R}(t)$ is the 3×3 rotation matrix describing the relative orientation between the left and right markers, and $\hat{T}(t)$ is the 3×1 vector describing the relative translation between the left and right markers. The angle of rotation can then be described as:

$$\hat{\theta}(t) = 2 * \sin\left(\sqrt{\hat{q}_x^2(t) + \hat{q}_y^2(t) + \hat{q}_z^2(t)}\right)$$

where $(\hat{q}_w(t), \hat{q}_x(t), \hat{q}_y(t), \hat{q}_z(t))^T$ is the unit quaternion representation of $\hat{R}(t)$ and $\hat{q}_w(t)$ is the scalar component of the quaternion.

If the relative pose between the left and right markers has been measured by a reference system and represented as:

$${}_{Left} H_{Right} = \begin{bmatrix} R & T \\ 0 & 1 \end{bmatrix} = \begin{bmatrix} I & T \\ 0 & 1 \end{bmatrix}$$

then the position error at time t can be defined as:

$$e_{p(t)} = \|\hat{T}(t)\| - \|T\|$$

and the orientation error at time t can be defined as:

$$e_{o(t)} = \hat{\theta}(t) - 0 = \hat{\theta}(t)$$

Statistics on these errors include:

Root mean square	RMS	$\sqrt{\frac{1}{N} \sum_{t=1}^N e_t^2}$
Maximum error	e_{max}	$\max(e_1 , e_2 , \dots, e_N)$
Percentile error	$E(p)$	$\begin{cases} E_k + d(E_{k+1} - E_k), & 0 < k < N \\ E_1, & k = 0 \\ E_N, & k \geq N \end{cases}$

Here, e_t denotes either the positional error $e_{p(t)}$ or the orientation error $e_{o(t)}$. In addition, the percentile error $E(p)$ on the ordered set $\{E_1, E_2, \dots, E_N\}$ is constructed from rearranging the set of errors $\{|e_1|, |e_2|, \dots, |e_N|\}$ by increasing value. Moreover,

$$\frac{p}{100}(N+1) = k + d$$

where k is an integer and $0 \leq d < 1$. The specific percentile errors reported are $E(99.7)$, $E(95)$, and $E(50)$.

EXPERIMENTS

Experiments were performed to first test the motion of optical tracking system camera mounts and then to test the ASTM E3064 standard test method. Optical tracking system camera mounting is critical to providing the best system calibration possible. If there is camera motion, the system measurement will provide less certainty than with fixed camera mounts. Hence, a measurement of camera motion is useful to determine how much motion the reference frame (including all cameras) provides. The authors measured the motion of two cameras mounted in worst-case locations for the reader to further understand this concept.

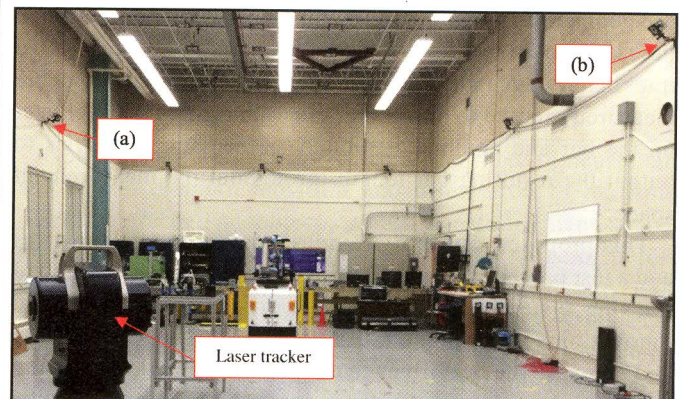


Figure 3. Laser tracker measuring a laboratory (a) outside-wall mount that supports an optical tracking system camera; (b) at right is the inside-wall mount that was measured

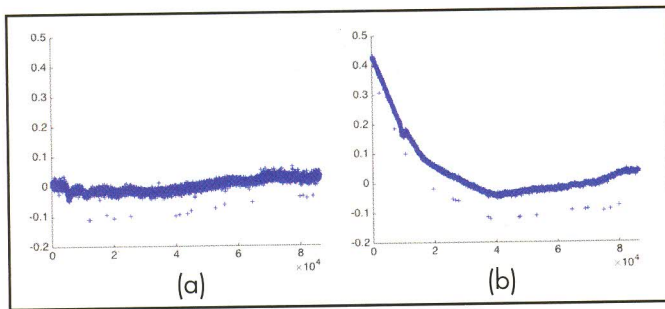


Figure 4. Laser tracker data from measurement of two camera mounts supporting optical tracking system cameras inside the laboratory on (a) an inside block wall and (b) an outside block wall; the horizontal axis is in sample points, and the vertical axis is in mm

For the first experiment, two optical tracking system camera mounts were each tracked for 24 hours using a laser tracker with an uncertainty of approximately $10 \mu\text{m}$.¹¹ Magnetic retroreflector mounts were glued to the two camera mounts located near the center of the longest walls of the rectangular laboratory. The laboratory, seen in figure 3, has 12 optical tracking system cameras mounted at a height of 4.3 m on 6.7 m-high perimeter walls. The laser tracker was programmed to take a data point each second for a total of 86,400 data points. The inside laboratory environment remained at a relatively constant room temperature and humidity. However, during the outside-wall motion measurement, the outside temperature changed by approximately 30°F between day and night. The day was overcast with a high of approximately 55°F . The optical tracking system calibration in the second experiment, however, was not performed during the same day as the first experiment because the laser tracker beam would have been obstructed during calibration and the experiment.

Before the second experiment, an optical tracking system calibration routine was performed. The routine included ensuring that extraneous reflectors were covered. These included a set of 13 covered reflectors, mounted on the perimeter walls for automatic guided vehicle (AGV) navigation. The AGV with onboard robot arm, including reflective markers detectable by the optical tracking system, were also covered with a large sheet of black plastic. In addition, the floor was covered with black plastic due to reflections onto the floor tile caused by infrared light-emitting diodes surrounding each camera. When the reflections were minimized, the tracking system was calibrated by waving the manufacturer's cali-

bration wand throughout the work volume until the system termed the calibration as "exceptional," meaning that there was a high confidence in the calibration.

The second experiment used the artifact seen at the top of figure 1a. The paths seen in figure 1b were then walked at an estimated

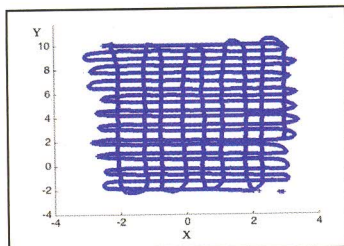


Figure 5. Sample data plot of the X and Y tracked paths of the artifact center

LENGTH						
Test	No. of samples	RMSD, deg.	Max, mm.	50 percentile, deg.	95 percentile, deg.	99.7 percentile, deg.
Length 1	86,617	0.532	31.804	0.15	0.606	2.068
Length 2	84,892	0.499	30.933	0.136	0.633	2.152
ANGLE						
Test	No. of samples	RMSD, deg.	Max, deg.	50 percentile, deg.	95 percentile, deg.	99.7 percentile, deg.
Angle 1	86,311	0.349	28.545	0.262	0.565	1.305
Angle 2	84,751	0.334	44.819	0.159	0.569	1.415

Figure 6. Table showing experimental results from the two trials

speed of $1.2 \text{ m/s} \pm 0.7 \text{ m/s}$ (as noted by the standard) over an area of approximately $13,000 \text{ mm} \times 6,000 \text{ mm}$ while the optical tracking system tracked the artifact motion. The artifact was held at a height of approximately 2 m and oriented as seen in figure 2a. This test area is similar to the third test volume described in the "Metrics and Test Method" section of this article. After both X and Y paths were walked with the artifact in the first artifact orientation, the experiment was repeated with the artifact held in the orientations seen in figure 2b and figure 2c. The data were then combined into a single data set, as required in the standard, and analyzed. The test method was then repeated for a second trial on another day after recalibration to ensure that the second experiment was properly performed and that the data retrieved were similar to the first day of the second experiment. The total time expended in the second experiment was approximately 12 minutes.

EXPERIMENTAL RESULTS

For the first experiment, the laser tracker provided results over 24 hours where, as expected, the inside wall moved much

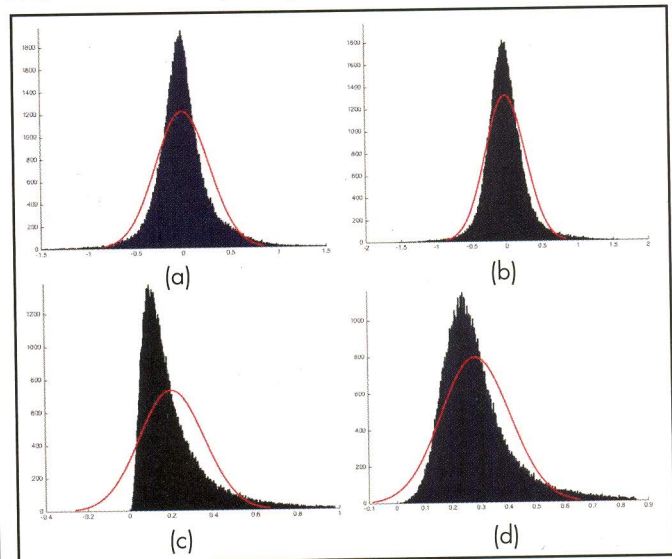


Figure 7. Histogram plots of the 99.7th percentile data shown in the table seen in figure 6 for (a) length from Trial 1; (b) length from Trial 2; (c) angle from Trial 1; and (d) angle from Trial 2; the Gaussian distribution in red is shown for comparison

less than the outside wall. The data are seen in figure 4 for both wall measurements.

For example, disregarding outliers, wall motion data spanned between approximately +0.04 mm and -0.05 mm for the inside wall, and between approximately +0.43 mm and -0.05 mm maximum for the outside wall. Outside wall measurement began at 2 p.m. Most motion of the outside wall occurred between 2 p.m. and 2 a.m., as seen in the left side of figure 4b. The optical tracking data captured for the second experiment and for calibration were collected over a period of only approximately 30 minutes each. Therefore, the motion of the walls during these periods was approximately 0.02 mm for the inside wall and 0.04 for the outside wall.

A sample data plot of the *X* and *Y* tracked paths can be seen in figure 5. The plot is of data collected from walking with the artifact in the vertical orientation (as seen in figure 2b) during the second trial. The results of the second experiment can be seen in the table in figure 6, for the two trials including analyzed data from both the artifact bar length and angle between artifact end-markers. The root mean square deviation (RMSD) shows approximately 0.5 mm length difference from the actual 300 mm length and approximately 0.34° difference from 0° actual angle. The maximum error, 50th percentile, 95th percentile, and 99.7th percentile length and angle results can also be seen.

The percentile error is listed in the ASTM E3064 standard, as opposed to the standard deviation, since the data distribution may not be Gaussian. Histogram plots of the 99.7th percentile distribution can be seen in figure 7. As seen, the length data are relatively evenly distributed, whereas the angle data are shifted positive.

CONCLUSIONS

Optical tracking systems are used in a wide range of fields and have dramatically grown in market share over the past several years. As such, a team of optical tracking system manufacturers, users, and researchers who were part of an ASTM E57.02 task group developed a standard test method (ASTM E3064). Toward completion of the standard, the test method procedures within the standard were tested in the two experiments described in this article. The theoretical basis for data analysis was also described, followed by analysis of the experimental data using this method. This work verified the performance of a 12-camera optical tracking system with an artifact, developed at NIST and measured previously using a CMM. Experimental results showed that the test method provides an RMSD of approximately 0.5 mm length difference from the actual 300 mm length and approximately 0.34° difference from 0° actual angle. Also, the use of percentiles vs. standard deviation was verified through histogram plots resulting in offset from the mean. To ensure that the optical tracking system was mounted and calibrated properly, a high-accuracy laser tracker was used to verify that the system camera mounts moved only slightly (i.e., approximately 0.02 mm for the inside wall and 0.04 for the outside wall) relative to the artifact RMSD results. Additionally, a system calibration was performed prior to each experiment. Future optical

tracking system standard efforts will be focused on system latency and perhaps other dynamic measurement performance characteristics.

ACKNOWLEDGEMENTS

The authors would like to thank the hard work and dedication of the ASTM E57.02 subcommittee task group for developing the E3064 standard. We also thank Dan Sawyer and his team from the NIST Dimensional Metrology Group for helping to develop and test the artifact.

REFERENCES

- ¹ Warren, W. H., Kay, B. A., Zosh, W. D., Duchon, A. P., and Sahuc, S., "Optic Flow Is Used to Control Human Walking", *Nature Neuroscience*, Vol. 4, No. 2, pp. 213–216, 2001.
- ² "OptiTrack for Movement Sciences," www.optitrack.com/motion-capture-movement-sciences, 2016.
- ³ Bostelman, R., Falco, J., Shah, M., and Hong, T., "Dynamic Metrology Performance Measurement of a Six Degree-of-Freedom Tracking System Used in Smart Manufacturing," *ASTM International STP1594: Autonomous Industrial Vehicles: From the Laboratory to the Factory Floor*, Ch. 7, pp. 91–105, 2016.
- ⁴ Shackleford, W., Cheok, G., Hong, T.-H., Saidi, K., and Shneier, M., "Performance Evaluation of Human Detection Systems for Robot Safety," *Journal of Intelligent & Robotic Systems*, Jan. 2016.
- ⁵ "Motion Capture Software Developers in the U.S.: Market Research Report," *IBIS World*, 2014.
- ⁶ Moeslund, T. B., Hilton, A., and Krüger, V., "A Survey of Advances in Vision-Based Human Motion Capture and Analysis," *Computer Vision and Image Understanding*, Vol. 104, No. 2, 2006.
- ⁷ Field, M., Stirling, D., Naghdy, F., and Pan, Z., "Motion Capture in Robotics Review," *6th IEEE International Conference on Control & Automation*, New Zealand, Dec. 2009.
- ⁸ ASTM E2919-14, www.astm.org/Standards/E2919.htm.
- ⁹ ASTM E3064 — "Standard Test Method for Evaluating the Performance of Optical Tracking Systems that Measure Six Degrees of Freedom (6DOF) Pose," www.astm.org, 2016.
- ¹⁰ English, C., Okouneva, G., Saint-Cyr, P., Choudhury, A., and Luu, T., "Real-Time Dynamic Pose Estimation Systems in Space: Lessons Learned for System Design and Performance Evaluation," *International Journal of Intelligent Control and Systems (IJICS)*, Vol. 16, No. 2, 2011.
- ¹¹ Burge, J. H., Su, P., Zhao, C., and Zobrist, T., "Use of a Commercial Laser Tracker for Optical Alignment," *Optical Engineering + Applications*, pp. 66760E–66760E, International Society for Optics and Photonics, 2007.